Title: Pattern-informed energetics: Energy allocation modeling for predicting trait variation and population persistence

Short running title: Modelling energetics in populations with PIE

Authors: Cara A. Gallagher[1,2*], Viktoriia Radchuk[3], Melanie Dammhahn[4,5], & Florian Jeltsch[1]

[1]Plant Ecology and Nature Conservation, Institute of Biochemistry and Biology, University of Potsdam, 14469 Potsdam, Germany.

[2]Department of Ecoscience, Aarhus University, 4000 Roskilde, Denmark.

[3]Leibniz Institute for Zoo and Wildlife Research, Alfred-Kowalke-Straße 17, Berlin, Germany.

[4]Behavioural Biology, Institute for Neuro- and Behavioural Biology, University of Münster, Badestrasse 9, 48149 Münster, Germany

[5]Joint Institute for Individualisation in a Changing Environment (JICE), University of Münster and Bielefeld University, Germany

Emails: cara.gallagher@ecos.au.dk; radchuk@izw-berlin.de; mdammhah@uni-muenster.de; jeltsch@uni-potsdam.de

Key words: Life history trade-offs, Bioenergetics, Ecological forecasting, Predictive ecology, Species persistence, Pace of life, Agent-based model, Individual-based model

Article type: Method

Word counts: Abstract (150); Main text (5017)

Count references: 85

Count figures: 5

***Corresponding author:** Cara Gallagher; Frederiksborgvej 399, 4000 Roskilde, Denmark; cara.gallagher@ecos.au.dk; +45 50190332

Data accessibility statement: All data, code, and materials used in the analyses are made available for download on Figshare at: Gallagher, Cara (2025). Pattern-informed energetics: Energy allocation modeling for predicting trait variation and population persistence. figshare. Dataset. https://doi.org/10.6084/m9.figshare.28390238.v1

Author contributions:

Conceptualization: CAG, VR, MD, FJ

Data curation: CAG

Methodology: CAG, VR, MD, FJ

Formal analysis: CAG

Visualization: CAG

Funding acquisition: FJ

Supervision: FJ

Writing—original draft: CAG

Writing—review & editing: CAG, VR, MD, FJ

Abstract

Energetics drive emergent ecosystem processes, shaping behavior and population dynamics in response to environmental conditions. While energy budget models can be used to effectively link resource dynamics to fitness outcomes, they often lack empirical grounding for energy allocation under resource constraints. Here, we introduce the Pattern-Informed Energetics (PIE) framework, which leverages diverse observations to infer parameters governing energy allocation. Using a rodent case study, we informed and tested PIE against 40 observed patterns, including population dynamics, morphometrics, energetics, and life-history traits, assessing its ability to replicate experimental results and predict responses to climate scenarios. Our findings demonstrate that PIE can predict how environmental change affects traits and population trajectories, offering a robust framework for improving biodiversity forecasting. By linking energy allocation to emergent patterns, PIE strengthens the integration of physiological insights into predictive models, improving our understanding of species' responses to environmental change while accounting for their evolved life histories.

Introduction

Amid unprecedented environmental change, accurately forecasting biodiversity responses is essential for understanding and managing ecosystem dynamics. Despite extensive effort, species declines and ecosystem disruptions persist (Ceballos et al., 2017). Predictive models can guide conservation by identifying drivers of change, prioritizing actions, and maximizing the use of limited resources (Dietze, 2017; Urban et al., 2016). However, model accuracy remains limited by gaps in understanding the processes driving species and ecosystem dynamics (Pilowsky et al., 2022). Given the diverse, multiscale, and nonlinear disruptions humans elicit in nature (Gilman et al., 2010), process-explicit models that integrate ecological theory with empirical data are essential for improving predictions and informing policy (Johnston et al., 2019; Urban et al., 2022).

Energy balance is a fundamental process shaping animal survival, reproduction, and population (Sibly et al., 2013; Burger et al., 2021) and community dynamics (Szangolies et al., 2024). Environmental change can disrupt energy acquisition and allocation, potentially compromising fitness (e.g., Clairbaux et al., 2021). In life-history theory, animal metabolisms are viewed as evolutionary adaptations tailored to specific environments, wherein the allocation of limited resources among survival, activity, growth, and reproduction is constrained by trait trade-offs (Ricklefs & Wikelski, 2002; White et al., 2022). Understanding these trade-offs can improve predictions of population responses to environmental stressors (Sibly et al., 2013).

Energy budget models have been applied for over 70 years to address diverse questions, from fisheries management to climate impacts on wildlife (Boyd et al., 2018; Desforges et al., 2021; Winberg, 1956). Approaches vary in their assumptions about allocation—from hierarchical prioritization (Sibly et al., 2013) to fixed fractions in Dynamic Energy Budget theory (Kooijman, 2000) and optimization-based strategies (McNamara & Houston, 1996)—but their relative predictive performance remains under-evaluated. While models inevitably simplify nature, integrating empirical observations into mechanistic projections can improve our understanding of population responses and guide strategies to mitigate biodiversity loss.

Technological advancements provide unprecedented insights into animal physiology, morphology, and demography, offering opportunities to refine energy budget models (e.g., Chimienti et al., 2020). Approaches such as pattern-oriented modeling (POM) and statistical inference (Gallagher et al., 2021; Grimm & Railsback, 2012; Hartig et al., 2011) allow for the derivation of key energetic parameters that are currently difficult or impossible to measure empirically, reducing reliance on arbitrary thresholds or assumptions of optimal behavior. A key gap remains in understanding how suboptimal energy intake influences allocation between competing demands of survival, activity, reproduction, and growth (McHuron et al., 2022; Pontzer & McGrosky, 2022; Sibly et al., 2013). Observing allocation processes *per se* remain infeasible, and even related empirical patterns, such as reproduction performance, remain scarce (but see Beltran et al., 2023; Bright Ross et al., 2021; Christiansen et al., 2014; Van Benthem et al., 2017). Yet, diverse existing patterns can inform energy allocation dynamics without relying on threshold-based or optimality assumptions. Statistical inference and POM can help uncover the context-dependent relationships governing energy allocation while accounting for the inherent uncertainty and variation within and between species.

Here, we introduce the Pattern-Informed Energetics (PIE) framework (Figure 1B), an energy budget modeling approach that derives context-dependent energy allocation strategies directly from empirical patterns, improving ecological realism. PIE provides mechanistic insights into the emergence of trait variation, driven by phenotypic plasticity, competitive interactions, and natural selection, and predicts population-level responses to environmental change. This approach allows for allocation strategies to emerge from the patterns they drive, such as morphometrics and growth, reproductive investment and success, and population dynamics. We illustrate the PIE framework using a bioenergetic model for terrestrial homeotherms, with bank vole (*Myodes glareolus*) populations as a case study. Using Approximate Bayesian Computation (ABC) for inverse parameterization, we derive allocation strategies and validate the model with POM by replicating an empirical litter manipulation experiment (Figure 1A). We then apply PIE to forecast population responses under future environmental scenarios using the Normalized Difference

Vegetation Index (NDVI) as a proxy for food availability (Tucker & Sellers, 1986). By leveraging diverse empirical knowledge to infer the values of parameters that shape some of the most elusive yet vital energetic processes driving animal fitness (McHuron et al., 2022; Sibly et al., 2013), the PIE approach can shed light on the driving forces behind the evolution of life history strategies and offers potential for improved predictive power.

Materials and methods

Model description

PIE provides a flexible, data-driven framework for simulating wildlife energetics within a dynamic, spatially explicit environment. It reveals how variation in morphology, metabolism, and life-history traits can emerge from underlying energy allocation strategies. While the conceptual approach for defining energy allocation curves is broadly applicable, model parameterization and validation are based on empirical data from bank voles, with the presented energy budget model, incorporating PIE, transferable to other terrestrial mammals.

A full TRACE document, including an ODD protocol (Grimm et al., 2014, 2020; Schmolke et al., 2010), sensitivity analyses, and calibration details, is available as supplemental material. The model is freely available at https://doi.org/10.6084/m9.figshare.28390238.v1.

Developed in NetLogo v6.2.0 (https://ccl.northwestern.edu/netlogo/), the model simulates interactions between animal agents and a 20x50-cell toroidal landscape. Each 10m×10m cell may contain food resources which replenish over time, with energy content and dry mass informed by vole forage data. The model runs on a 30-minute timestep during the active breeding season (day 90–273), excluding winter due to its relatively limited influence on key processes.

The model includes two entities: landscape cells and animal agents. Animals are characterized by dynamic state variables tracking morphometrics, energy dynamics, and reproduction, with only female adults modeled. Each timestep involves: (1)

movement decisions, (2) energetic costs, (3) resource consumption, and (4) updates to tissue stores, reproduction, and survival.

Movement is represented implicitly, with animals moving at speeds drawn from a gamma distribution fitted to empirical data. Although movement is not spatially tracked, its consequences are modeled through foraging cell selection and transport costs.

Energy expenditure is calculated sequentially across maintenance, transport, reproduction, and lean mass growth (Figure 1B). Maintenance costs scale allometrically with body mass, while locomotion costs include both postural and speed-related components. Reproductive costs cover pregnancy and lactation, based on allocation curves and maternal condition. Lean mass deposition includes structural growth and protein use for metabolic costs, with realized growth also determined using allocation curves.

Food intake is shaped by energy demand, stomach capacity, hunger, body condition, and local resource availability. Animals attempt to ingest food to offset their energy shortfall, constrained by stomach volume and clearance rates. Digestive capacities adjust dynamically—especially during lactation—to reflect increased energy needs, consistent with empirical data. Hunger is modeled using dual-intervention theory (Speakman, 2014): increasing at low body fat, decreasing at high body fat, and remaining stable at intermediate levels.

After foraging, animals update their energy balance and adjust tissue stores. Surpluses lead to lean and fat mass deposition, while deficits trigger catabolism. Tissue dynamics follow Forbes' theory (Forbes, 2009), where protein use/deposition increases as body fat decreases, and are grounded in rodent data. Mortality risk, including starvation and abortion, is assessed daily based on energy stores. Reproductive events are triggered by calendar day and reproductive status. At year-end, overwinter mortality occurs, and resource levels are reset.

Model calibration

Twelve uncertain parameters were calibrated using POM. Calibration occurred in two stages: (1) resource parameters were adjusted to match empirical bank vole population densities, and (2) ten sigmoidal parameters shaping allocation curves linking body condition to growth, reproduction, and survival were determined using 16 empirical patterns.

To ensure realistic abundances, maximum resource levels (g/cell) and accumulation rates (g/timestep) were tested across 25 simulations, with densities compared to several empirical studies. The best-fitting combination minimized the mean absolute deviation from the median empirical density (14.2 voles/ha).

To explore the influence of body condition on energy allocation and survival, we used rejection approximate Bayesian computation (ABC) (van der Vaart et al., 2016) to test 500,000 parameter combinations shaping energy allocation and survival curves. Model outputs were compared to 16 empirical patterns, with error assessed using R statistical software (R Core Team, 2021). The 30 best-fitting parameter sets were retained to balance accuracy and uncertainty (Boult et al., 2019; van der Vaart et al., 2016).

Evaluation

After calibration, we assessed the model's ability to replicate the results of an empirical litter manipulation experiment (Koivula et al., 2003), which examined the effects of manipulated litter size on weanling number, body mass, subsequent breeding attempts, and maternal survival in wild bank voles over three years (1996–1998) in Konnevesi, Finland. Litter manipulation is a classic life-history research method where litter sizes are experimentally altered in females post-birth to explore the costs and trade-offs of reproduction (Koivula et al., 2003; Koskela, 1998; Oksanen et al., 2001).

We replicated resource conditions at the experimental site using the NDVI3g dataset (1990–1999), interpolated to daily resolution. A linear relationship between NDVI and food availability was adopted as a pragmatic solution in lieu of empirical data defining these dynamics. NDVI values (0-1) were scaled to a 0–2 modifier for

maximum resource levels, where 1 maintained the calibrated value, 0 reduced resources to zero, and 2 was double the calibrated value. Pregnant females were assigned to 'Enlarged' (+2 pups), 'Reduced' (−2 pups), or 'Control' groups. We tracked population abundance and 12 patterns related to birth, weaning, and reproduction (13 patterns total; Table S8.2). To account for stochasticity, we ran 100 simulation replicates, with outputs analyzed in R following empirical results.

As a more general evaluation, we compared model outputs to an additional 11 independent empirical patterns (Table S8.1). Outputs from 150 simulations were collected at the end of the fifth simulation year, with further tracking into the sixth year for survival rates. Visual comparisons assessed model agreement with empirical data.

Scenario details

To assess the model's ability to project trait variation and population trajectories, we ran future simulations for Konnevesi, Finland again using NDVI-driven resource dynamics. We collected data on 13 individual traits (energetics, morphometrics, reproduction) and population abundance, either seasonally or annually, under historical and projected resource dynamics. These predictions are not absolute forecasts due to the exclusion of factors like predation and site-specific resource availability (food items, energy densities, etc.). Instead, they illustrate the model's capacity to reveal how resource dynamics drive trait variation and population dynamics, mediated through individual energy dynamics.

NDVI data was obtained from the Terra MODIS mission (MOD13Q1; Didan, 2021) at 250m spatial and 16-day temporal resolution (2000-2022) for a 4 km^2 area at the study site (62°37'N, 26°17'E), accessed via the MODISTools package in R (Tuck et al., 2014). NDVI values were averaged for each observation day to capture seasonal dynamics and incorporated into the model as in the litter manipulation experiment (see 'Evaluation').

Projections through 2099 were generated using a linear mixed-effects model with mean NDVI as the response variable and monthly temperature, and precipitation as

predictors. Fixed effects included linear and quadratic terms for precipitation and minimum temperature, with random intercepts for year to account for annual variability. More complex models (including solar radiation and lagged predictors) did not significantly improve fit (assessed via AIC and R^2), so we proceeded with the simpler model. Projected monthly minimum temperature and precipitation data came from three Global Climate Models (GCMs) (CNRM-CM6-1-HR, EC-Earth3-CC, AWI-CM-1-1-MR; Döscher et al., 2022; Semmler et al., 2018; Voldoire, 2019) under SSP245, SSP585, and historical emissions scenarios from the Coupled Model Intercomparison Project Phase 6 (CMIP6) accessed via the Copernicus Climate Data Store (https://cds.climate.copernicus.eu/).

To better capture within-year NDVI dynamics, we explored alternative scenarios projecting average annual NDVI while simulating within-annual changes using randomly selected years from observed data. Projections were interpolated to daily NDVI changes and averaged across the three GCMs, producing one projection per emissions scenario.

We ran simulations for three scenarios (two emissions scenarios: SSP245, SSP585; two projection approaches for SSP585) for 100 years with 500 repetitions to account for stochasticity from ABC parameter combinations and other sources. Six observation days per year (two each in spring, summer, and fall) were used to observe all relevant agents. Thirteen traits were recorded for 2018-2022 (observed) and 2094-2098 (projected), with population abundance collected on each observation day from 2018-2099.

Six traits (body mass, body condition, field metabolic rate, locomotion costs, energy allocation to reproduction/growth) were averaged for adults (>45 days old). Three traits (litter size, body mass of neonates/pups) were collected for events between observations and assigned to the next observation day. The final four traits (lifetime reproductive success, age at first birth, number of litters, age at death) were updated at parturition or death and averaged annually. Body mass, metabolic rate, and energy allocation reflect immediate physiological responses, while lifetime reproductive success and longevity provide insights into life-history traits.

Outcomes were analyzed using R, calculating mean and coefficient of variation for each output across observed and projected periods. Within-year dynamics were visualized using generalized additive models, while across-year trends and trait-population relationships were explored with linear models. Pearson correlation coefficients (*r*) were calculated for 171 trait-population combinations (mean and CV of 13 traits and six outcomes; df = 498) to identify general trends for each period. Though we did not examine how trait-population relationships change within or between years, the model allows for such analyses.

Results

Calibration of population densities, energy allocation, and survival

Model calibration for realistic vole densities resulted in maximum resource levels of 140 g/grid cell and accumulation rates of 0.011 g/timestep, yielding 14.4 ± 13.7 females/hectare, peaking in mid-summer (empirical mean: 17.5 ± 11.8 females/hectare; TRACE Section 6.1).

Using inverse parameterization with ABC and POM (TRACE Section 6.2), we found outputs from the 30 best-performing parameter combinations to closely match empirical patterns (Figure 2A-M), with minor discrepancies primarily attributed to conflicts between patterns. Posterior distributions were substantially narrowed, effectively identifying a subset of plausible values consistent with observations (TRACE Figure S6.4). However, parameters representing curve slopes showed less reduction. Further analysis showed that these parameters were positively correlated with their corresponding midpoints (e.g., the slope and midpoint shaping the growth allocation curve; TRACE Figure S6.5), indicating they were difficult to estimate independently, with slope variation having less impact on outputs than midpoints.

The 30 selected parameter combinations were used in simulations (Figure 2N-P), with variation across runs to account for uncertainty.

Model evaluation and replication of a litter manipulation experiment

Model outputs closely aligned with 13 observed patterns from the empirical litter manipulation experiment (Figure 3), demonstrating strong agreement across multiple ecological and life-history dimensions. Seasonal population density dynamics were accurately captured, including mid-summer peaks and year-specific variations such as higher early-summer densities in 1997 (Figure 3A). The model also effectively replicated declines in weanling body mass due to both seasonality and litter size manipulation (Figure 3B), with offspring mass at weaning reduced in Enlarged litters, highlighting its ability to capture how maternal investment and environmental conditions influence offspring growth. Litter size at weaning followed observed seasonal trends, with the largest litters in mid-summer and smallest in late summer (Figure 3C). Female survival patterns were also well represented, with lowest survival in late summer and among females with enlarged litters (Figure 3D).

Some discrepancies remained, particularly in the relationship between birth litter size and litter size at weaning. While the model successfully predicted smaller weaned litters for reduced litters, as observed, it tended to overestimate litter size at weaning overall and failed to reflect that larger birth litters did not lead to larger weaned litters, particularly in early- and mid-summer. These differences may reflect underlying biological processes not explicitly represented in the current model structure, such as preferential feeding or infanticide. Nevertheless, the weaker correlation in late summer mirrored the observed pattern of more consistent litter sizes across manipulation groups.

Additional tests against independent empirical data on energy dynamics, survival, life history, and morphometrics further supported model accuracy (TRACE Section 8.1). Field metabolic rates and food consumption across age classes aligned closely with findings from nine separate studies. These patterns reflect emergent total metabolisms shaped by behavior, energy costs, and allocation strategies, making the strong agreement especially encouraging.

Scenarios of resource variation impacts on individual traits and population dynamics

Scenarios revealed strong seasonal and interannual variation in population density. Under historical conditions (2018–2022), populations peaked in late summer, with occasional early summer peaks. Under projected conditions (2094–2098), densities followed similar trends but with higher peak values.

Correlations between traits and population metrics revealed distinct patterns (Figure 5G). Under observed conditions, maximum offspring abundance (A_{peak}) was negatively correlated with storage levels (SL) (r = -0.54, 95%CI: [−0.60,−0.48]; Figure 5D) and offspring mass at weaning (m_{wean}) (r = -0.65, 95%CI: [−0.70,−0.59]). Timing of peak adult (T_{Apeak}) and offspring (T_{Opeak}) abundance were negatively correlated with locomotion costs (M_L) and age at first birth ($age_{1st\ birth}$) (T_{Apeak}-M_L: r = -0.64, 95%CI: [−0.69,−0.59]; T_{Apeak}-$age_{1st\ birth}$: r = -0.72, 95%CI: [−0.76,−0.68]; T_{Opeak}-M_L: r = -0.50, 95%CI: [−0.57,−0.43]; T_{Opeak}-$age_{1st\ birth}$: r = -0.84, 95%CI: [−0.87,−0.82]). Positive correlations were observed between the peak adult (A_{peak}) and offspring (O_{peak}) abundance and longevity (age_{death}) (A_{peak}-age_{death}: r = 0.61, 95%CI: [0.55,0.66] (Figure 5C); O_{peak}-age_{death}: r = 0.55, 95%CI: [0.48,0.60]), as well as between the timing of minimum adult abundance (T_{Amin}) and age at first birth ($age_{1st\ birth}$) (r = 0.56, 95%CI: [0.50,0.62]).

Under projected conditions, most correlations remained, with slightly stronger effects across all output combinations (sum absolute *r*: Historic: 52.9; Projected: 56.0) (Figure 5H). Timing-related population metrics (T_{Apeak}, T_{Opeak}, and T_{Amin}) showed the greatest increases. The strong negative correlation between minimum adult abundance (A_{min}) and total metabolic rate (M_{tot}) held across both time periods (Projected: r = -0.55, 95%CI: [-0.61,-0.48]; Figure 5F), related to trends with allocation to reproduction (M_R) and lean mass deposition (M_{LM}) (A_{min}-M_R: r = -0.52, 95%CI: [-0.58,-0.45]; A_{min}-M_{LM}: r = -0.49, 95%CI: [-0.55,-0.42]). Strong positive relationships between peak adult (A_{peak}) and offspring (O_{peak}) abundance and litter size at weaning (LSW) and lifetime reproductive success (LRS) also remained across periods (Projected: A_{peak}-LSW: r = 0.80, 95%CI: [0.77,0.83] (Figure 5E); A_{peak}-LRS: r = 0.79, 95%CI: [0.75,0.82]; O_{peak}-LSW: r = 0.71, 95%CI: [0.67,0.75]; O_{peak}-LRS: r = 0.57, 95%CI: [0.51,0.63]). All

correlations described here were significant ($p < 0.001$, $n = 500$ per combination). See Appendix Figures A2 and A3 for full correlation matrices.

The model predicted a slight increase in population density throughout the century (Historical: 15.7 ± 2.0; Projected: 16.8 ± 2.7 female voles/hectare; Figure 5C). In alternative scenarios which retained observed within-year NDVI dynamics, correlations were slightly weaker (sum absolute *r*: 52.0; Figure A4), but population densities increased to 18.5 ± 2.8 females/hectare. Under the SSP245 scenario, correlation patterns remained similar, with stable population densities (Projected: 15.2 ± 2.1 females/hectare; Figure A5).

Discussion

1830/1800 words

Allocation remains among the most daunting energetic processes to measure empirically (McHuron et al., 2022; Sibly et al., 2013). Using a PIE approach, we successfully informed allocation dynamics by applying inverse parameter estimation, leveraging patterns in morphometrics, energy expenditure, and life history which emerge from allocation processes. This approach allowed allocation to be dynamic and incorporate uncertainty, producing model outputs that reliably matched observations. Notably, the model successfully recreated complex empirical patterns in morphometrics, reproduction, survival, and density under conditions mimicking a field experiment, demonstrating its predictive power for real-world biological processes. By addressing key uncertainties in energetics, this approach can improve predictions of organismal responses to environmental change, particularly those affecting foraging efficiency and resource dynamics.

Individual-based bioenergetic models are increasingly used for predicting ecological responses to change (Pirotta, 2022; Rose et al., 2024). The PIE approach can strengthen these models by tailoring energy allocation dynamics to species-specific information, making it particularly valuable for applied contexts such as conservation

and management. Beyond applied uses, PIE can also provide insights into fundamental ecological and evolutionary questions, including the emergence and consequences of individual variation (Bolnick et al., 2011; Dammhahn et al., 2018). By integrating plasticity and dynamic variation in energetics, morphometrics, and life history traits, the approach directly links these traits to resource environments. Since allocation strategies may be shaped by selection, influencing pace-of-life differences across and potentially within species (Stearns, 1989, 2000), extensions investigating eco-evolutionary dynamics could offer valuable insights into the role of resource dynamics in selection processes. Moreover, its grounding in first principles allows for assessing the combined effects of multiple, co-occurring environmental changes (Orr et al., 2020; Pirotta et al., 2022).

When replicating conditions of the real-world experiment in Koivula et al. (2003), the model effectively reproduced field observations and provided a mechanistic explanation for its successes and limitations. Notably, it excelled in predicting seasonal dynamics, showing lower averages for litter size, offspring mass, litter mass at weaning, and female survival in late summer, consistent with reproductive trade-offs under resource limitation and high population densities (Koivula et al., 2003; Koskela, 1998). It also captured allocation-driven trends, such as reduced survival and smaller weaning masses in females with enlarged litters. However, the model failed to fully capture the common finding that larger birth litters do not yield more weaned offspring (Koskela, 1998; Mappes et al., 1995; Oksanen et al., 2001). Although females with enlarged litters had lower offspring survival, this effect was too weak to equalize weaned litter sizes. This gap may reflect unmodeled maternal behaviors, such as selective feeding or infanticide. Additionally, weaned litter sizes were generally larger than observed, likely due to missing non-energetic factors like predation and dispersal (Mazurkiewicz & Rajska, 1975). Despite this, the model successfully captured complex seasonal and experimental dynamics, demonstrating that its implemented mechanisms can reproduce high-level ecological patterns.

When applied to scenarios, the model demonstrated how changes in individual traits due to environmental shifts relate to broader ecological patterns, such as adult and offspring abundance, timing of population peaks, and reproductive success. While

causal relationships were not assessed here due to matters of design, these could be explored in future studies. The model highlighted key factors shaping ecological responses, such as correlations between body mass and peak abundance, and reproductive costs influencing the timing of population fluctuations. Life-history traits like longevity, lifetime reproductive success, and litter size at weaning typically corresponded with higher abundances but were often negatively associated with morphometric and energetic factors, such as body mass and total metabolic costs, and age at first birth.

Interestingly, although an inverse relationship between body mass and peak abundance aligns with broader mass–abundance patterns—where resource limitations cap total biomass or individual numbers (Damuth, 1981, 1987; Scheffer, 1955), cyclical rodents like bank voles often show increased body size during population peaks, a phenomenon known as the Chitty effect (Chitty & Chitty, 1962). This effect, associated with higher survival and suppressed reproduction, is thought to result from energy being redirected toward growth (Johannesen & Andreassen, 2008; Oli, 1999) and may be heritable (Sundell et al., 2019). Although the model did not produce true population cycles, it showed that increased longevity was associated with higher peak abundances. The absence of cyclical dynamics likely reflects missing drivers such as shifts in energy allocation, predation, dispersal, and social interactions (e.g. Radchuk et al., 2016). However, the model's mechanistic flexibility makes it well-suited for testing alternative hypotheses and exploring the conditions under which cycles might emerge, with detailed consideration of energetic factors.

By bridging micro-level processes (e.g., energy expenditure and morphometrics) with macro-level patterns (e.g., population density), this approach advances understanding of how individual responses to environmental variability drive broader shifts in population dynamics. Research indicates that physiological constraints shape life history strategies both across (Healy et al., 2019) and within (Burton et al., 2011) species, with trait-demography relationships documented in small mammals and seabirds (Jenouvrier et al., 2015, 2018; Van Benthem et al., 2017). This approach provides a mechanistic understanding of these trait correlations, shedding light on

the resource-driven pathways linking environmental change to population outcomes (Manzo, 2022). Moreover, findings suggest potential conservation implications, such as the association between higher locomotive costs and reduced peak population abundance. In European brown hares (*Lepus europaeus*), increased activity behavior, and consequently higher locomotive costs, have been linked to changes in resource dynamics (Ullmann et al., 2018). The model's results suggest that such impacts could relate to a decline in adult abundance.

Model projections suggest population density will increase with rising resource availability, forecasting a 7.0% rise in average annual density and a 13.1% increase in peak abundance by century's end. However, NDVI rose by 21.5% over this period, indicating that resource and population responses are not strictly proportional. While NDVI is a common proxy for resource availability (Boult et al., 2019; Howard et al., 2024; Karunarathna et al., 2024), it doesn't always reflect consumable resources. Despite this, it remains valuable for capturing seasonality and relative differences. The choice of an appropriate proxy should depend on study objectives and system-specific considerations, with alternatives including the Enhanced Vegetation Index (Huete et al., 2002), precipitation, or direct food availability measures (Howard et al., 2024). Other ecological drivers, such as masting events (Reil et al., 2015), predation (Radchuk et al., 2016), interspecific competition (Eccard & Ylönen, 2002, 2003), and habitat structure (Ecke et al., 2002), also shape vole populations but were excluded here for model tractability. Future studies aiming for absolute predictions should integrate empirical data on these factors. Additionally, while the three selected GCMs provided high-resolution climate projections, they represent only a subset of available CMIP6 models (Eyring et al., 2016).

The PIE framework itself relies on key assumptions. Grounding allocation dynamics in empirical patterns supports model realism but assumes those patterns accurately represent system function. However, measurement error, study conditions, and sample size can all affect the accuracy and transferability of empirical patterns (Gallagher et al., 2021). Addressing these challenges requires integrating multiple patterns across ecological levels, as done here (Gallagher et al., 2021; Grimm & Railsback, 2012). Tools like the virtual ecologist approach (Zurell et al., 2010) can help

reduce biases by simulating outputs under conditions comparable to observations. Additionally, while patterns are treated as static, they often depend on local context (e.g., habitat, climate, species interactions) and may shift through plasticity, adaptation, or evolution (Edelaar & Bolnick, 2019). For long-term forecasts, incorporating adaptive and evolutionary dynamics may be essential (Wortel et al., 2023). Ideally, understanding how patterns vary over time and space would refine model processes, but in lieu of such rare data, using diverse empirical patterns can still support realistic model behavior (Grimm, 2005).

Understanding ecological systems requires models that incorporate assumptions and imperfect data, but the urgency of environmental change demands that we make full use of available tools and knowledge to address emerging threats and safeguard biodiversity (Mouquet et al., 2015; Urban et al., 2016). Energy forms a fundamental link between environmental conditions and animal fitness. As such, advances in empirical knowledge of physiology and energy allocation can improve how models capture physiological and life history diversity (e.g. White et al., 2022). While such improvements increase realism, they also introduce complexity, which is unnecessary for some questions, but essential for others requiring detailed links between environments and fitness. The predictive value of the PIE approach has yet to be tested against alternative frameworks (e.g., Kooijman, 2000; Mangel, 2015; Sibly et al., 2013), and more broadly, few comparisons exist among current energy allocation models. Additionally, trade-offs in metabolism and energy allocation remain poorly resolved, particularly regarding plasticity and the drivers of intake and expenditure (Halsey, 2018, 2021; Laskowski et al., 2021; Speakman, 2014). The model presented here offers a platform to explore these dynamics, but robust inter-model comparisons—supported by statistical validation and multivariate spatiotemporal data—are needed to assess predictive gains (Pilowsky et al., 2022). Determining when detailed energetic modeling is necessary for accurate forecasts can help advance predictive ecology.

The fundamental concept of the PIE framework, where energy allocation curves are informed by empirical patterns, is not limited to the specific model presented here. It can be incorporated into other bioenergetic modeling approaches (e.g., Kooijman,

2000; Sibly et al., 2013), guiding allocation based on nutritional status in a way that reflects observed patterns. By leveraging empirical patterns, researchers can avoid *ad hoc* approaches to inform energy allocation dynamics, making PIE a valuable approach for researchers developing bioenergetic models. Moreover, the presented energy budget model is transferable to other terrestrial homeotherms, given sufficient data, though movement processes may need adaptation for non-central place foragers. In applying the approach to new systems, we suggest using patterns in relationships between energy demand, intake, and body condition, with outcomes measured via morphometrics, reproduction, and survival. Emerging empirical methods are increasingly capturing relevant patterns, enhancing the PIE framework's applicability. For instance, recent studies link body condition and mass gain to reproductive performance in species like polar bears (*Ursus maritimus*), badgers (*Meles meles*), and elephant seals (*Mirounga angustirostris*) (Archer et al., 2023; Beltran et al., 2023; Bright Ross et al., 2021). These advances provide directly applicable patterns for PIE that offer immense potential for improving the realism and accuracy of bioenergetic models.

Conclusion

Although the direct measurement of energy allocation processes remains challenging, the PIE framework offers a robust alternative by leveraging empirical patterns to inform these processes in predictive models. This approach enables dynamic allocation, incorporates uncertainty, and enhances model realism. By accurately reproducing a wide range of observed patterns (40 in total), the model shows promise for both theoretical and applied ecology. Though not without limitations, the PIE framework is adaptable and well-suited to predicting individual and population responses to environmental change. Integration with existing modeling methods, supported by growing empirical datasets, can greatly improve bioenergetics modeling and deepen ecological understanding. Applying the PIE approach at the community level may also help reveal species interactions and energy flows, offering powerful insights into biodiversity and ecosystem responses, insights that are increasingly critical in the face of ongoing and accelerating environmental change.

Acknowledgements

We extend our gratitude to Victoria Boult for valuable early discussions that contributed to the development of scenarios. Additionally, we thank Herman Pontzer for his insightful discussions on modeling animal energy budgets and allocation, which greatly inspired this work. Funding for this study was provided by the DFG-funded research training group 'BioMove' (Deutsche Forschungsgemeinschaft Grant GRK 2118) (CAG, VR, MD, FJ).

References

Archer, L., Atkinson, S., Pagano, A., Penk, S., & Molnár, P. (2023). Lactation performance in polar bears is associated with fasting time and energetic state. *Marine Ecology Progress Series*, *720*, 175–189. https://doi.org/10.3354/meps14382

Beltran, R. S., Hernandez, K. M., Condit, R., Robinson, P. W., Crocker, D. E., Goetsch, C., Kilpatrick, A. M., & Costa, D. P. (2023). Physiological tipping points in the relationship between foraging success and lifetime fitness of a long-lived mammal. *Ecology Letters*, *26*(5), 706–716. https://doi.org/10.1111/ele.14193

Bolnick, D. I., Amarasekare, P., Araújo, M. S., Bürger, R., Levine, J. M., Novak, M., Rudolf, V. H. W., Schreiber, S. J., Urban, M. C., & Vasseur, D. A. (2011). Why Intraspecific Trait Variation Matters in Community Ecology. *Trends in Ecology & Evolution*, *26*(4), 183–192. https://doi.org/10.1016/j.tree.2011.01.009

Boult, V. L., Fishlock, V., Quaife, T., Hawkins, E., Moss, C., Lee, P. C., & Sibly, R. M. (2019). Human-driven habitat conversion is a more immediate threat to Amboseli elephants than climate change. *Conservation Science and Practice*, *1*(9). https://doi.org/10.1111/csp2.87

Boyd, R., Roy, S., Sibly, R., Thorpe, R., & Hyder, K. (2018). A general approach to incorporating

spatial and temporal variation in individual-based models of fish populations with application to Atlantic mackerel. *Ecological Modelling*, *382*, 9–17. https://doi.org/10.1016/j.ecolmodel.2018.04.015

Bright Ross, J. G., Newman, C., Buesching, C. D., Connolly, E., Nakagawa, S., & Macdonald, D. W. (2021). A fat chance of survival: Body condition provides life-history dependent buffering of environmental change in a wild mammal population. *Climate Change Ecology*, *2*, 100022. https://doi.org/10.1016/j.ecochg.2021.100022

Burton, T., Killen, S. S., Armstrong, J. D., & Metcalfe, N. B. (2011). What causes intraspecific variation in resting metabolic rate and what are its ecological consequences? *Proceedings of the Royal Society B: Biological Sciences*, *278*(1724), 3465–3473. https://doi.org/10.1098/rspb.2011.1778

Ceballos, G., Ehrlich, P. R., & Dirzo, R. (2017). Biological annihilation via the ongoing sixth mass extinction signaled by vertebrate population losses and declines. *Proceedings of the National Academy of Sciences*, *114*(30), E6089–E6096. https://doi.org/10.1073/pnas.1704949114

Chimienti, M., Desforges, J.-P., Beumer, L. T., Nabe-Nielsen, J., van Beest, F. M., & Schmidt, N. M. (2020). Energetics as common currency for integrating high resolution activity patterns into dynamic energy budget-individual based models. *Ecological Modelling*, *434*, 109250. https://doi.org/10.1016/j.ecolmodel.2020.109250

Chitty, H., & Chitty, D. (1962). Body weight in relation to population phase in Microtus agrestis. *Symp. Theriologicum, Brno*, *1960*, 77–86.

Christiansen, F., Víkingsson, G. A., Rasmussen, M. H., & Lusseau, D. (2014). Female body condition affects foetal growth in a capital breeding mysticete. *Functional Ecology*, *28*(3), 579–588. https://doi.org/10.1111/1365-2435.12200

Clairbaux, M., Mathewson, P., Porter, W., Fort, J., Strøm, H., Moe, B., Fauchald, P., Descamps, S., Helgason, H. H., & Bråthen, V. S. (2021). North Atlantic winter cyclones starve seabirds. *Current Biology: CB*, *31*(17), 3964–3971.

Dammhahn, M., Dingemanse, N. J., Niemelä, P. T., & Réale, D. (2018). Pace-of-life syndromes: A framework for the adaptive integration of behaviour, physiology and life history. *Behavioral Ecology and Sociobiology*, *72*(3), 62. https://doi.org/10.1007/s00265-018-2473-y

Damuth, J. (1981). Population density and body size in mammals. *Nature*, *290*(5808), 699–700. https://doi.org/10.1038/290699a0

Damuth, J. (1987). Interspecific allometry of population density in mammals and other animals: The independence of body mass and population energy-use. *Biological Journal of the Linnean Society*, *31*(3), 193–246. https://doi.org/10.1111/j.1095-8312.1987.tb01990.x

Desforges, J.-P., Beest, F. M. van, Marques, G. M., Pedersen, S. H., Beumer, L. T., Chimienti, M., & Schmidt, N. M. (2021). Quantifying energetic and fitness consequences of seasonal heterothermy in an Arctic ungulate. *Ecology and Evolution*, *11*(1), 338–351. https://doi.org/10.1002/ece3.7049

Didan, K. (2021). *MOD13Q1 MODIS/Terra Vegetation Indices 16-Day L3 Global 250m SIN Grid V061* [Dataset]. https://doi.org/10.5067/MODIS/MOD13Q1.061

Dietze, M. C. (2017). Prediction in ecology: A first-principles framework. *Ecological Applications*, *27*(7), 2048–2060. https://doi.org/10.1002/eap.1589

Döscher, R., Acosta, M., Alessandri, A., Anthoni, P., Arsouze, T., Bergman, T., Bernardello, R., Boussetta, S., Caron, L.-P., Carver, G., Castrillo, M., Catalano, F., Cvijanovic, I., Davini, P., Dekker, E., Doblas-Reyes, F. J., Docquier, D., Echevarria, P., Fladrich, U., … Zhang, Q. (2022). The EC-Earth3 Earth system model for the Coupled Model Intercomparison Project 6. *Geoscientific Model Development*, *15*(7), 2973–3020. https://doi.org/10.5194/gmd-15-2973-2022

Eccard, J. A., & Ylönen, H. (2002). Direct interference or indirect exploitation? An experimental study of fitness costs of interspecific competition in voles. *Oikos*, *99*(3), 580–590. https://doi.org/10.1034/j.1600-0706.2002.11833.x

Eccard, J. A., & Ylönen, H. (2003). Who Bears the Costs of Interspecific Competition in an Age-Structured Population? *Ecology*, *84*(12), 3284–3293. https://doi.org/10.1890/02-0220

Ecke, F., Löfgren, O., & Sörlin, D. (2002). Population dynamics of small mammals in relation to forest age and structural habitat factors in northern Sweden. *Journal of Applied Ecology*, *39*(5), 781–792. https://doi.org/10.1046/j.1365-2664.2002.00759.x

Edelaar, P., & Bolnick, D. I. (2019). Appreciating the Multiple Processes Increasing Individual or Population Fitness. *Trends in Ecology & Evolution*, *34*(5), 435–446. https://doi.org/10.1016/j.tree.2019.02.001

Eyring, V., Bony, S., Meehl, G. A., Senior, C. A., Stevens, B., Stouffer, R. J., & Taylor, K. E. (2016). Overview of the Coupled Model Intercomparison Project Phase 6 (CMIP6) experimental design and organization. *Geoscientific Model Development*, *9*(5), 1937–1958. https://doi.org/10.5194/gmd-9-1937-2016

Forbes, G. B. (2009). Lean Body Mass-Body Fat Interrelationships in Humans. *Nutrition Reviews*, *45*(10), 225–231. https://doi.org/10.1111/j.1753-4887.1987.tb02684.x

Gallagher, C. A., Chudzinska, M., Larsen-Gray, A., Pollock, C. J., Sells, S. N., White, P. J. C., & Berger, U. (2021). From theory to practice in pattern-oriented modelling: Identifying and using empirical patterns in predictive models. *Biological Reviews*, *96*(5), 1868–1888. https://doi.org/10.1111/brv.12729

Gilman, S. E., Urban, M. C., Tewksbury, J., Gilchrist, G. W., & Holt, R. D. (2010). A framework for community interactions under climate change. *Trends in Ecology & Evolution*, *25*(6), 325–331. https://doi.org/10.1016/j.tree.2010.03.002

Grimm, V. (2005). Pattern-Oriented Modeling of Agent-Based Complex Systems: Lessons from Ecology. *Science*, *310*(5750), 987–991. https://doi.org/10.1126/science.1116681

Grimm, V., Augusiak, J., Focks, A., Frank, B. M., Gabsi, F., Johnston, A. S. A., Liu, C., Martin, B. T., Meli, M., Radchuk, V., Thorbek, P., & Railsback, S. F. (2014). Towards better modelling and decision support: Documenting model development, testing, and analysis using TRACE. *Ecological Modelling*, *280*, 129–139.

https://doi.org/10.1016/j.ecolmodel.2014.01.018

Grimm, V., & Railsback, S. F. (2012). Pattern-oriented modelling: A 'multi-scope' for predictive systems ecology. *Philosophical Transactions of the Royal Society B: Biological Sciences*, *367*(1586), 298–310. https://doi.org/10.1098/rstb.2011.0180

Grimm, V., Railsback, S. F., Vincenot, C. E., Berger, U., Gallagher, C., DeAngelis, D. L., Edmonds, B., Ge, J., Giske, J., Groeneveld, J., Johnston, A. S. A., Milles, A., Nabe-Nielsen, J., Polhill, J. G., Radchuk, V., Rohwäder, M.-S., Stillman, R. A., Thiele, J. C., & Ayllón, D. (2020). The ODD Protocol for Describing Agent-Based and Other Simulation Models: A Second Update to Improve Clarity, Replication, and Structural Realism. *Journal of Artificial Societies and Social Simulation*, *23*(2), 7. https://doi.org/10.18564/jasss.4259

Halsey, L. G. (2018). Keeping Slim When Food Is Abundant: What Energy Mechanisms Could Be at Play? *Trends in Ecology & Evolution*, *33*(10), 745–753. https://doi.org/10.1016/j.tree.2018.08.004

Halsey, L. G. (2021). The Mystery of Energy Compensation. *Physiological and Biochemical Zoology*, 716467. https://doi.org/10.1086/716467

Hartig, F., Calabrese, J. M., Reineking, B., Wiegand, T., & Huth, A. (2011). Statistical inference for stochastic simulation models - theory and application: Inference for stochastic simulation models. *Ecology Letters*, *14*(8), 816–827. https://doi.org/10.1111/j.1461-0248.2011.01640.x

Healy, K., Ezard, T. H. G., Jones, O. R., Salguero-Gómez, R., & Buckley, Y. M. (2019). Animal life history is shaped by the pace of life and the distribution of age-specific mortality and reproduction. *Nature Ecology & Evolution*, *3*(8), 1217–1224. https://doi.org/10.1038/s41559-019-0938-7

Howard, C., Mason, T. H. E., Baillie, S. R., Border, J., Hewson, C. M., Houston, A. I., Pearce-Higgins, J. W., Bauer, S., Willis, S. G., & Stephens, P. A. (2024). Explaining and predicting animal migration under global change. *Diversity and Distributions*, *30*(2), e13797. https://doi.org/10.1111/ddi.13797

Huete, A., Didan, K., Miura, T., Rodriguez, E. P., Gao, X., & Ferreira, L. G. (2002). Overview of the radiometric and biophysical performance of the MODIS vegetation indices. *Remote Sensing of Environment*, *83*(1), 195–213. https://doi.org/10.1016/S0034-4257(02)00096-2

Jenouvrier, S., Desprez, M., Fay, R., Barbraud, C., Weimerskirch, H., Delord, K., & Caswell, H. (2018). Climate change and functional traits affect population dynamics of a long-lived seabird. *Journal of Animal Ecology*, *87*(4), 906–920. https://doi.org/10.1111/1365-2656.12827

Jenouvrier, S., Péron, C., & Weimerskirch, H. (2015). Extreme climate events and individual heterogeneity shape life-history traits and population dynamics. *Ecological Monographs*, *85*(4), 605–624. https://doi.org/10.1890/14-1834.1

Johannesen, E., & Andreassen, H. P. (2008). Density-dependent variation in body mass of voles. *Acta Theriologica*, *53*(2), 169–173. https://doi.org/10.1007/BF03194249

Johnston, A. S. A., Boyd, R. J., Watson, J. W., Paul, A., Evans, L. C., Gardner, E. L., & Boult, V. L. (2019). Predicting population responses to environmental change from individual-level mechanisms: Towards a standardized mechanistic approach. *Proceedings of the Royal Society B: Biological Sciences*, *286*(1913), 20191916. https://doi.org/10.1098/rspb.2019.1916

Karunarathna, K. A. N. K., Wells, K., & Clark, N. J. (2024). Modelling nonlinear responses of a desert rodent species to environmental change with hierarchical dynamic generalized additive models. *Ecological Modelling*, *490*, 110648. https://doi.org/10.1016/j.ecolmodel.2024.110648

Koivula, M., Koskela, E., Mappes, T., & Oksanen, T. A. (2003). Cost of reproduction in the wild: Manipulation of reproductive effort in the bank vole. *Ecology*, *84*(2), 398–405. https://doi.org/10.1890/0012-9658(2003)084[0398:CORITW]2.0.CO;2

Kooijman, S. A. L. M. (2000). *Dynamic Energy and Mass Budgets in Biological Systems*. Cambridge University Press.

Koskela, E. (1998). Offspring growth, survival and reproductive success in the bank vole: A litter size manipulation experiment. *Oecologia*, *115*(3), 379–384.

https://doi.org/10.1007/s004420050531

Laskowski, K. L., Moiron, M., & Niemelä, P. T. (2021). Integrating Behavior in Life-History Theory: Allocation versus Acquisition? *Trends in Ecology & Evolution*, *36*(2), 132–138. https://doi.org/10.1016/j.tree.2020.10.017

Mangel, M. (2015). Stochastic Dynamic Programming Illuminates the Link Between Environment, Physiology, and Evolution. *Bulletin of Mathematical Biology*, *77*(5), 857–877. https://doi.org/10.1007/s11538-014-9973-3

Manzo, G. (2022). *Agent-based Models and Causal Inference*. John Wiley & Sons.

Mappes, T., Koskela, E., & Ylönen, H. (1995). Reproductive costs and litter size in the bank vole. *Proceedings of the Royal Society of London. Series B: Biological Sciences*, *261*(1360), 19–24. https://doi.org/10.1098/rspb.1995.0111

Mazurkiewicz, M., & Rajska, E. (1975). Dispersion of young bank voles from their place of birth. *Acta Theriologica*, *20*, 71–81. https://doi.org/10.4098/AT.arch.75-6

McHuron, E. A., Adamczak, S., Arnould, J. P. Y., Ashe, E., Booth, C., Bowen, W. D., Christiansen, F., Chudzinska, M., Costa, D. P., Fahlman, A., Farmer, N. A., Fortune, S. M. E., Gallagher, C. A., Keen, K. A., Madsen, P. T., McMahon, C. R., Nabe-Nielsen, J., Noren, D. P., Noren, S. R., … Williams, R. (2022). Key questions in marine mammal bioenergetics. *Conservation Physiology*, *10*(1), coac055. https://doi.org/10.1093/conphys/coac055

Mouquet, N., Lagadeuc, Y., Devictor, V., Doyen, L., Duputié, A., Eveillard, D., Faure, D., Garnier, E., Gimenez, O., Huneman, P., Jabot, F., Jarne, P., Joly, D., Julliard, R., Kéfi, S., Kergoat, G. J., Lavorel, S., Le Gall, L., Meslin, L., … Loreau, M. (2015). Predictive ecology in a changing world. *Journal of Applied Ecology*, *52*(5), 1293–1310. https://doi.org/10.1111/1365-2664.12482

Oksanen, T. A., Jonsson, P., Koskela, E., & Mappes, T. (2001). Optimal allocation of reproductive effort: Manipulation of offspring number and size in the bank vole. *Proceedings of the Royal Society of London. Series B: Biological Sciences*, *268*(1467), 661–666. https://doi.org/10.1098/rspb.2000.1409

Oli, M. K. (1999). The Chitty Effect: A Consequence of Dynamic Energy Allocation in a

Fluctuating Environment. *Theoretical Population Biology*, *56*(3), 293–300. https://doi.org/10.1006/tpbi.1999.1427

Orr, J. A., Vinebrooke, R. D., Jackson, M. C., Kroeker, K. J., Kordas, R. L., Mantyka-Pringle, C., Van den Brink, P. J., De Laender, F., Stoks, R., Holmstrup, M., Matthaei, C. D., Monk, W. A., Penk, M. R., Leuzinger, S., Schäfer, R. B., & Piggott, J. J. (2020). Towards a unified study of multiple stressors: Divisions and common goals across research disciplines. *Proceedings of the Royal Society B: Biological Sciences*, *287*(1926), 20200421. https://doi.org/10.1098/rspb.2020.0421

Pilowsky, J. A., Colwell, R. K., Rahbek, C., & Fordham, D. A. (2022). Process-explicit models reveal the structure and dynamics of biodiversity patterns. *Science Advances*, *8*(31), eabj2271. https://doi.org/10.1126/sciadv.abj2271

Pirotta, E. (2022). A review of bioenergetic modelling for marine mammal populations. *Conservation Physiology*, *10*(1), coac036. https://doi.org/10.1093/conphys/coac036

Pirotta, E., Thomas, L., Costa, D. P., Hall, A. J., Harris, C. M., Harwood, J., Kraus, S. D., Miller, P. J. O., Moore, M. J., Photopoulou, T., Rolland, R. M., Schwacke, L., Simmons, S. E., Southall, B. L., & Tyack, P. L. (2022). Understanding the combined effects of multiple stressors: A new perspective on a longstanding challenge. *Science of The Total Environment*, *821*, 153322. https://doi.org/10.1016/j.scitotenv.2022.153322

Pontzer, H., & McGrosky, A. (2022). Balancing growth, reproduction, maintenance, and activity in evolved energy economies. *Current Biology*, *32*(12), R709–R719. https://doi.org/10.1016/j.cub.2022.05.018

R Core Team. (2021). *R: A language and environment for statistical computing* [Computer software]. R Foundation for Statistical Computing. https://www.R-project.org/

Radchuk, V., Ims, R. A., & Andreassen, H. P. (2016). From individuals to population cycles: The role of extrinsic and intrinsic factors in rodent populations. *Ecology*, *97*(3), 720–732. https://doi.org/10.1890/15-0756.1

Reil, D., Imholt, C., Eccard, J. A., & Jacob, J. (2015). Beech Fructification and Bank Vole

Population Dynamics—Combined Analyses of Promoters of Human Puumala Virus Infections in Germany. *PLOS ONE*, *10*(7), e0134124. https://doi.org/10.1371/journal.pone.0134124

Ricklefs, R. E., & Wikelski, M. (2002). The physiology/life-history nexus. *Trends in Ecology & Evolution*, *17*(10), 462–468. https://doi.org/10.1016/S0169-5347(02)02578-8

Rose, K., Holsman, K., Nye, J., Markowitz, E., Banha, T., Bednaršek, N., Bueno-Pardo, J., Deslauriers, D., Fulton, E., Huebert, K., Huret, M., Ito, S., Koenigstein, S., Li, L., Moustahfid, H., Muhling, B., Neubauer, P., Paula, J., Siddon, E., … Peck, M. (2024). Advancing bioenergetics-based modeling to improve climate change projections of marine ecosystems. *Marine Ecology Progress Series*, *732*, 193–221. https://doi.org/10.3354/meps14535

Scheffer, V. B. (1955). Body Size with Relation to Population Density in Mammals. *Journal of Mammalogy*, *36*(4), 493–515. https://doi.org/10.2307/1375805

Schmolke, A., Thorbek, P., DeAngelis, D. L., & Grimm, V. (2010). Ecological models supporting environmental decision making: A strategy for the future. *Trends in Ecology & Evolution*, *25*(8), 479–486. https://doi.org/10.1016/j.tree.2010.05.001

Semmler, T., Danilov, S., Rackow, T., Sidorenko, D., Barbi, D., Hegewald, J., Sein, D., Wang, Q., & Jung, T. (2018). *AWI-CM-1.1-MR model output prepared for CMIP6 CMIP: Links to 1pctCO2, abrupt-4xCO2, historical, and piControl simulations* [Other]. Earth System Grid Federation; German Climate Computing Center (DKRZ). https://doi.org/10.22033/ESGF/CMIP6.359

Sibly, R. M., Grimm, V., Martin, B. T., Johnston, A. S. A., Kułakowska, K., Topping, C. J., Calow, P., Nabe-Nielsen, J., Thorbek, P., & DeAngelis, D. L. (2013). Representing the acquisition and use of energy by individuals in agent-based models of animal populations. *Methods in Ecology and Evolution*, *4*(2), 151–161. https://doi.org/10.1111/2041-210x.12002

Speakman, J. R. (2014). If Body Fatness is Under Physiological Regulation, Then How Come We Have an Obesity Epidemic? *Physiology*, *29*(2), 88–98.

https://doi.org/10.1152/physiol.00053.2013

Stearns, S. C. (1989). Trade-Offs in Life-History Evolution. *Functional Ecology*, *3*(3), 259–268. https://doi.org/10.2307/2389364

Stearns, S. C. (2000). Life history evolution: Successes, limitations, and prospects. *Naturwissenschaften*, *87*(11), 476–486. https://doi.org/10.1007/s001140050763

Sundell, J., Ylönen, H., & Haapakoski, M. (2019). Do phase-dependent life history traits in cyclic voles persist in a common environment? *Oecologia*, *190*(2), 399–410. https://doi.org/10.1007/s00442-019-04410-3

Szangolies, L., Gallagher, C. A., & Jeltsch, F. (2024). Individual energetics scale up to community coexistence: Movement, metabolism and biodiversity dynamics in fragmented landscapes. *Journal of Animal Ecology*, *93*(8), 1065–1077. https://doi.org/10.1111/1365-2656.14134

Tuck, S. L., Phillips, H. R. P., Hintzen, R. E., Scharlemann, J. P. W., Purvis, A., & Hudson, L. N. (2014). MODISTools – downloading and processing remotely sensed data in R. *Ecology and Evolution*, *4*(24), 4658–4668. https://doi.org/10.1002/ece3.1273

Tucker, C. J., & Sellers, P. J. (1986). Satellite remote sensing of primary production. *International Journal of Remote Sensing*, *7*(11), 1395–1416. https://doi.org/10.1080/01431168608948944

Ullmann, W., Fischer, C., Pirhofer-Walzl, K., Kramer-Schadt, S., & Blaum, N. (2018). Spatiotemporal variability in resources affects herbivore home range formation in structurally contrasting and unpredictable agricultural landscapes. *Landscape Ecology*, *33*(9), 1505–1517. https://doi.org/10.1007/s10980-018-0676-2

Urban, M. C., Bocedi, G., Hendry, A. P., Mihoub, J.-B., Peer, G., Singer, A., Bridle, J. R., Crozier, L. G., De Meester, L., Godsoe, W., Gonzalez, A., Hellmann, J. J., Holt, R. D., Huth, A., Johst, K., Krug, C. B., Leadley, P. W., Palmer, S. C. F., Pantel, J. H., … Travis, J. M. J. (2016). Improving the forecast for biodiversity under climate change. *Science*, *353*(6304), aad8466–aad8466. https://doi.org/10.1126/science.aad8466

Urban, M. C., Travis, J. M. J., Zurell, D., Thompson, P. L., Synes, N. W., Scarpa, A., Peres-Neto, P. R.,

Malchow, A.-K., James, P. M. A., Gravel, D., De Meester, L., Brown, C., Bocedi, G., Albert, C. H., Gonzalez, A., & Hendry, A. P. (2022). Coding for Life: Designing a Platform for Projecting and Protecting Global Biodiversity. *BioScience*, *72*(1), 91–104. https://doi.org/10.1093/biosci/biab099

Van Benthem, K. J., Froy, H., Coulson, T., Getz, L. L., Oli, M. K., & Ozgul, A. (2017). Trait–demography relationships underlying small mammal population fluctuations. *Journal of Animal Ecology*, *86*(2), 348–358. https://doi.org/10.1111/1365-2656.12627

van der Vaart, E., Johnston, A. S. A., & Sibly, R. M. (2016). Predicting how many animals will be where: How to build, calibrate and evaluate individual-based models. *Ecological Modelling*, *326*, 113–123. https://doi.org/10.1016/j.ecolmodel.2015.08.012

Voldoire, A. (2019). *CNRM-CERFACS CNRM-CM6-1-HR model output prepared for CMIP6 HighResMIP* [Dataset]. Earth System Grid Federation. https://doi.org/10.22033/ESGF/CMIP6.1387

White, C. R., Alton, L. A., Bywater, C. L., Lombardi, E. J., & Marshall, D. J. (2022). Metabolic scaling is the product of life-history optimization. *Science*, *377*(6608), 834–839. https://doi.org/10.1126/science.abm7649

Winberg, G. G. (1956). Rate of metabolism and food requirements of fishes. *Fish. Res. Bd. Canada Trans. Ser.*, *433*, 1–251.

Wortel, M. T., Agashe, D., Bailey, S. F., Bank, C., Bisschop, K., Blankers, T., Cairns, J., Colizzi, E. S., Cusseddu, D., Desai, M. M., van Dijk, B., Egas, M., Ellers, J., Groot, A. T., Heckel, D. G., Johnson, M. L., Kraaijeveld, K., Krug, J., Laan, L., … Pennings, P. S. (2023). Towards evolutionary predictions: Current promises and challenges. *Evolutionary Applications*, *16*(1), 3–21. https://doi.org/10.1111/eva.13513

Zurell, D., Berger, U., Cabral, J. S., Jeltsch, F., Meynard, C. N., Münkemüller, T., Nehrbass, N., Pagel, J., Reineking, B., Schröder, B., & Grimm, V. (2010). The virtual ecologist approach: Simulating data and observers. *Oikos*, *119*(4), 622–635. https://doi.org/10.1111/j.1600-0706.2009.18284.x

Figures

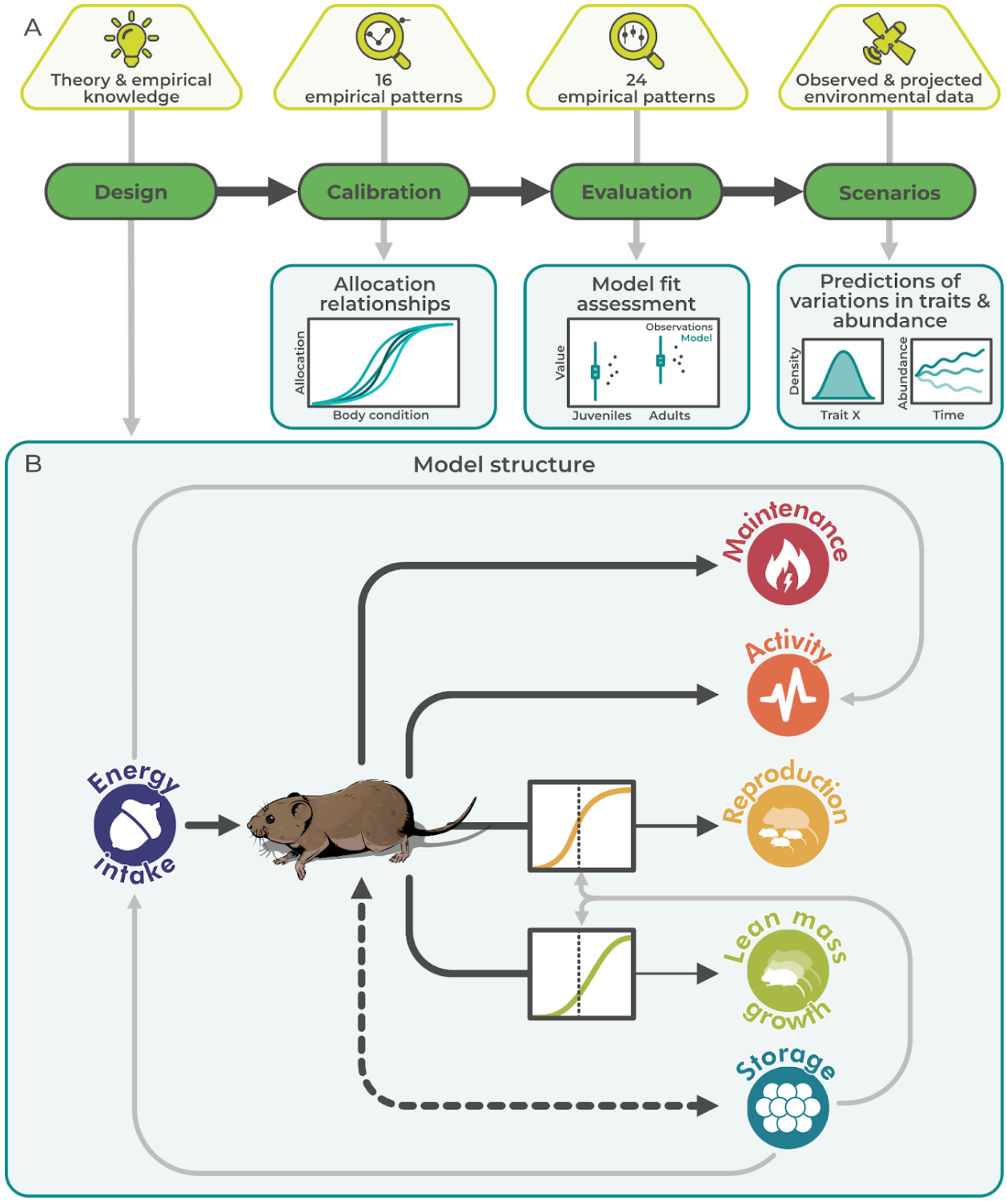
A
Theory & empirical knowledge
16 empirical patterns
24 empirical patterns
Observed & projected environmental data
Design
Calibration
Evaluation
Scenarios
Allocation relationships
Allocation
Body condition
Model fit assessment
Observations
Model
Value
Juveniles
Adults
Predictions of variations in traits & abundance
Density
Trait X
Abundance
Time
B
Model structure
Maintenance
Activity
Energy intake
Reproduction
Lean mass growth
Storage

Figure 1. A) Schematic representing key inputs and outputs of the model development, testing, and application process. B) Key processes underlying the energy budget framework, with light grey lines indicating interactions between processes. The sigmoidal functions associated with growth and reproduction represent the allocation of energy to these processes. Within the PIE approach, energy allocation is guided by body-condition-dependent relationships, which result from model calibration to empirical patterns.

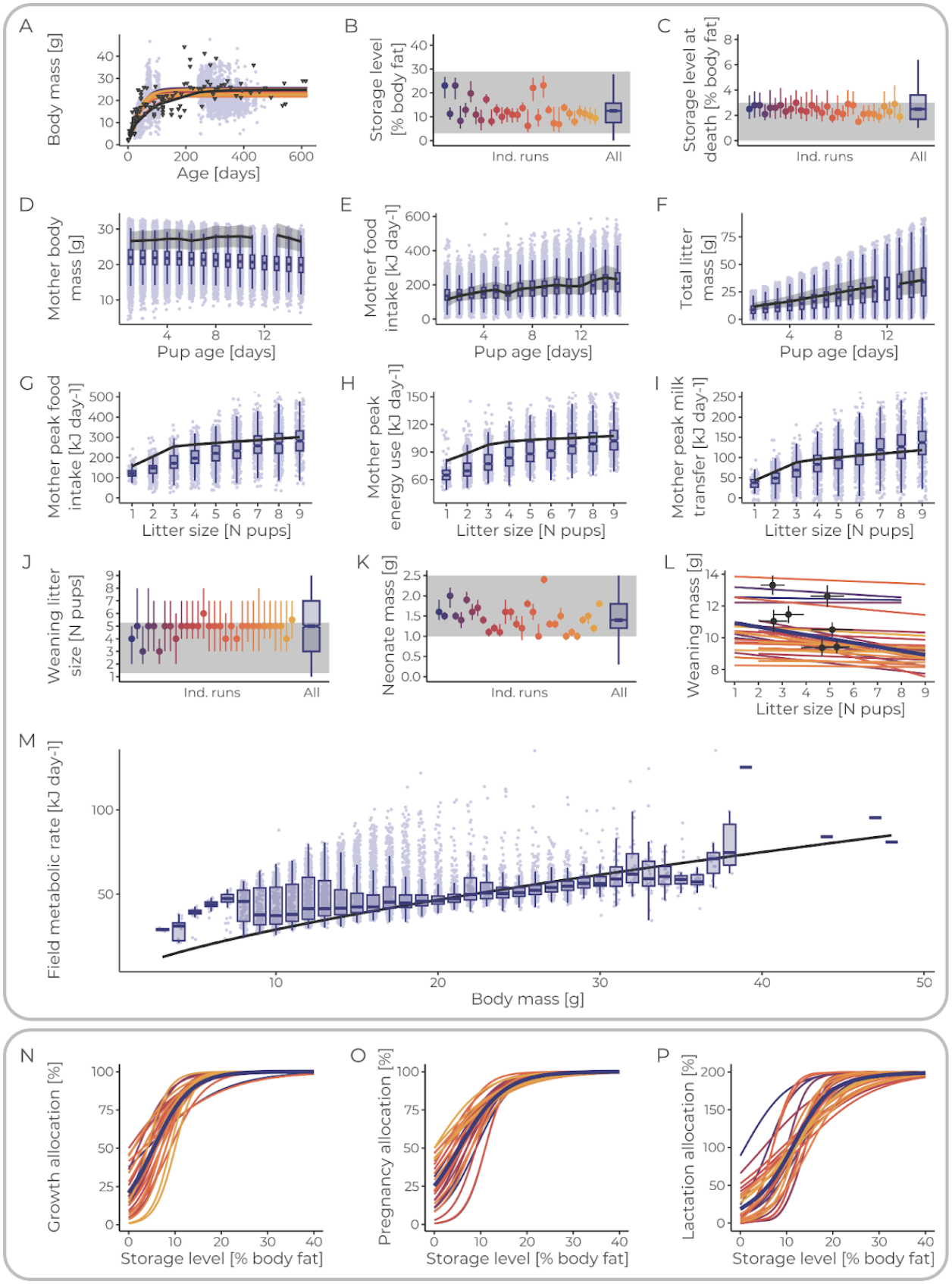
A
Body mass [g]
Age [days]
B
Storage level [% body fat]
Ind. runs
All
C
Storage level at death [% body fat]
Ind. runs
All
D
Mother body mass [g]
Pup age [days]
E
Mother food intake [kJ day-1]
Pup age [days]
F
Total litter mass [g]
Pup age [days]
G
Mother peak food intake [kJ day-1]
Litter size [N pups]
H
Mother peak energy use [kJ day-1]
Litter size [N pups]
I
Mother peak milk transfer [kJ day-1]
Litter size [N pups]
J
Weaning litter size [N pups]
Ind. runs
All
K
Neonate mass [g]
Ind. runs
All
L
Weaning mass [g]
Litter size [N pups]
M
Field metabolic rate [kJ day-1]
Body mass [g]
N
Growth allocation [%]
Storage level [% body fat]
O
Pregnancy allocation [%]
Storage level [% body fat]
P
Lactation allocation [%]
Storage level [% body fat]

Figure 2. Comparison of model predictions for the 30 best-fitting parameter combinations against the empirical patterns used for calibration (empirical data depicted in black or grey) for A) total body mass, B) percent body fat of living animals, and C) percent body fat at death, D) mother body mass and E) food intake, F) total litter mass with pup age, G) mother peak food intake, H) energy use, and I) milk transfer with litter size, J) litter size at weaning, K) neonate mass, L) weanling mass by litter size, and M) field metabolic rate of non-lactating animals by body mass. Outputs from individual parameter sets are shown in unique colors, with combined results in purple. Colored point ranges represent the median and 95% CIs for each individual parameter set, with light purple points in A, D-I, and M representing individual simulation data points. In panels B-F, J, and K, the grey rectangle indicates the range of empirical values used to assess pattern fit, while the grey shaded region in D-F represents the mean ± SE of the empirical data. For panels A, G, H, I, and M, empirical relations are shown as solid black lines. In panel L, fit was defined qualitatively as a negative relationship, with illustrative points (mean ± SE) from two independent empirical studies (Koskela, 1998; Oksanen et al., 2001). In panels A and L, colored lines represent von Bertalanffy and linear relationships fit to outputs for each parameter set. Panels N-P show the selected allocation relationships of the 30 best-fitting parameter sets, illustrating the association between body fat percentage and allocation to N) growth, O) pregnancy, and P) lactation. Approximate Bayesian computation (ABC) was used to evaluate 500,000 parameter combinations, assessing fit with median absolute scaled error for univariate or multivariate patterns and a pass/fail approach for linear relationships. See supplementary TRACE document section 6 “Model output verification” for more details and further patterns used in model development.

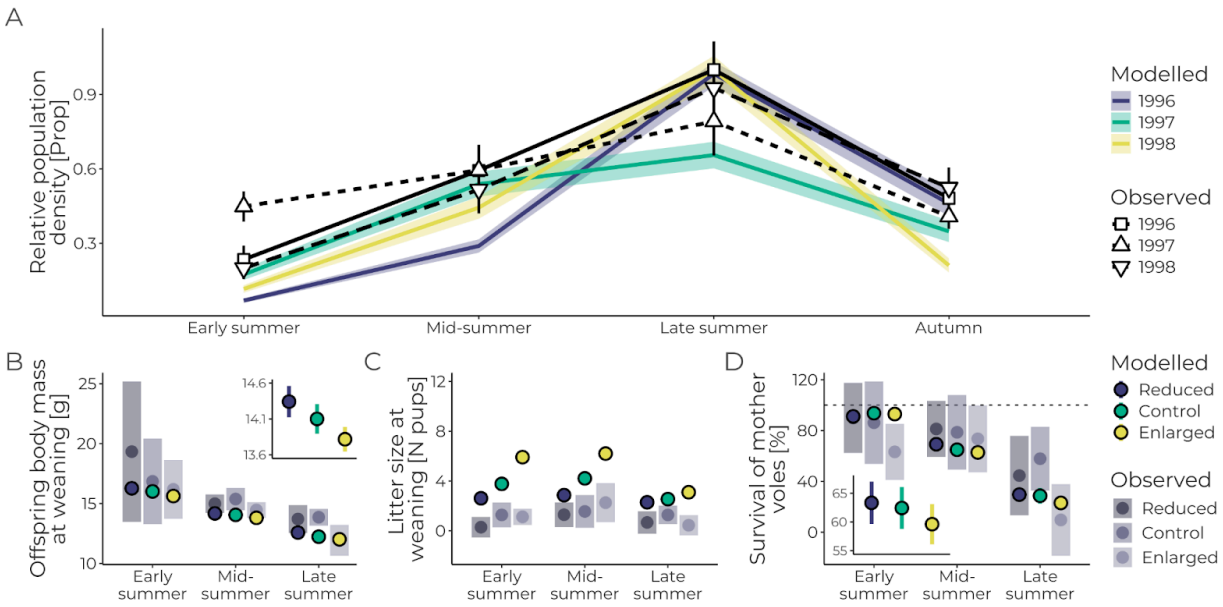

Figure 3. Comparison of model outputs with empirical data from the litter manipulation experiment in Konnevesi, Finland for 1996-1998 (Koivula et al. 2003). A) Seasonal population density dynamics per year (proportion of maximum value) (mean ± SE), B) offspring body mass (in grams) at weaning , C) litter size (count pups) at weaning , and D) mother survival (%) to the next breeding period (means ± 95% CIs). Insets panels in B and D display the seasonal averages (means ± 95% CIs), with the dotted line in panel D representing 100% survival. Predictions were generated from 100 simulation replicates. All observed estimates were taken directly from plots presented in Koivula et al. (2003).

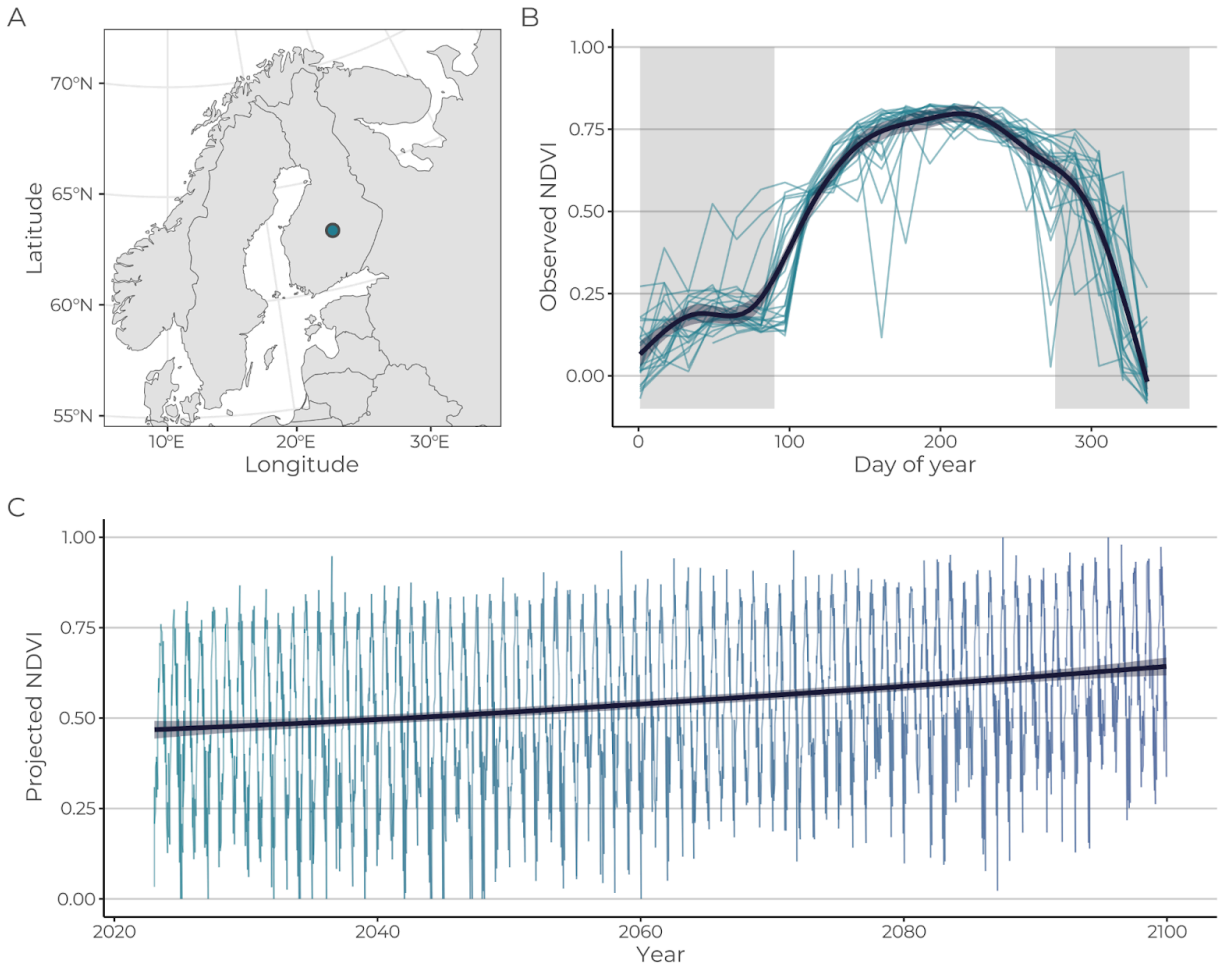

Figure 4. Characteristics of the site used for the replication of a real-world experiment in model evaluation and for scenario simulations in Konnevesi, Finland (A). For the scenarios, B) seasonal variations in observed resource dynamics, represented by NDVI, are shown with colored lines indicating individual years (2000–2022) that drove historical resource dynamics. C) Projected future resource dynamics under the SSP585 emissions scenario, generated based on projected temperature and precipitation changes. Dark lines in B and C represent GAM predictions.

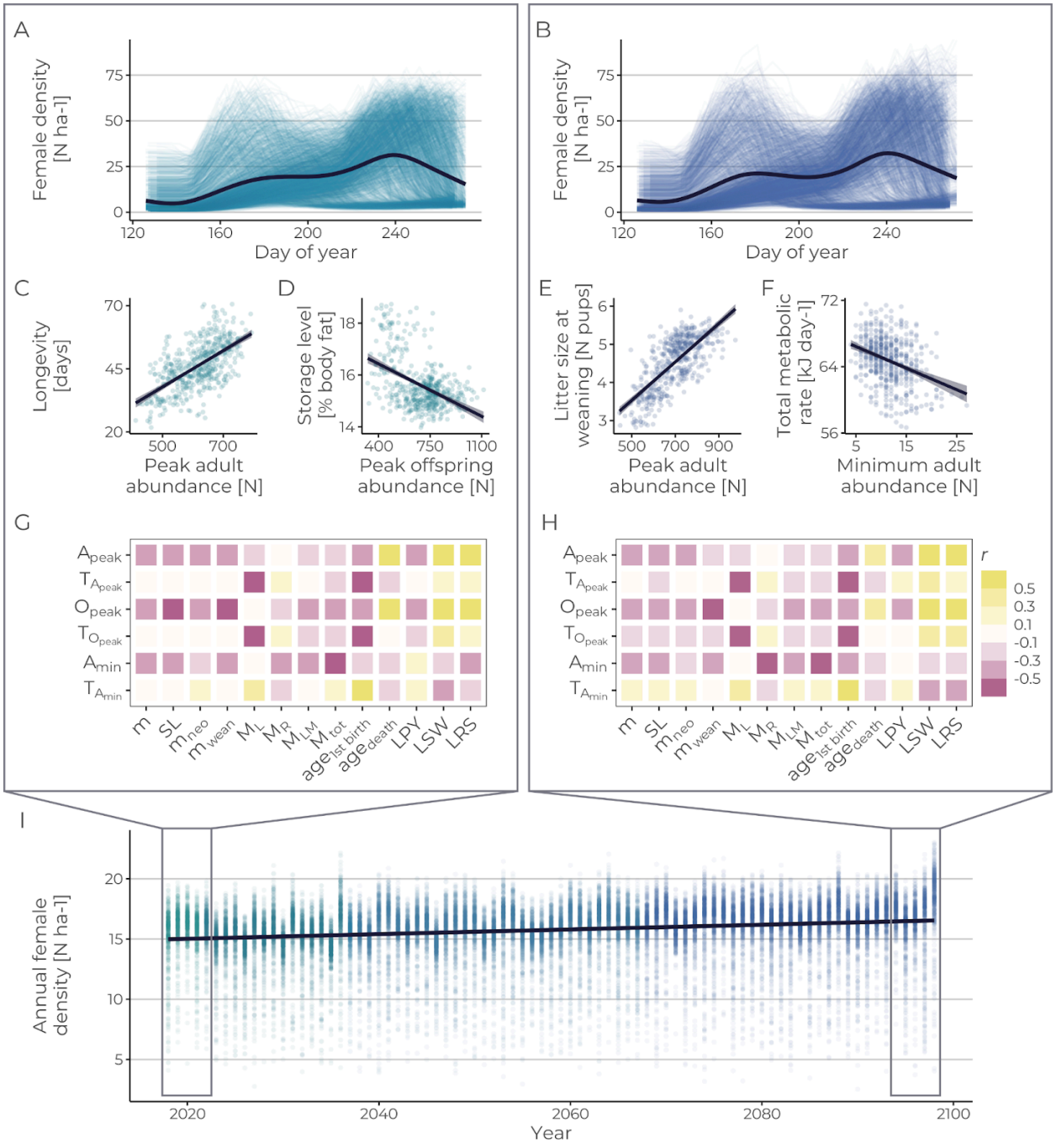

Figure 5. Predicted temporal variations in population dynamics, life history, and morphometric traits under observed and projected resource dynamics, based on the SSP585 emissions scenario. In A, C, D, and G, results are shown for 2018–2022, while B, E, F, and H depict results for 2094–2098. Changes in annual averages of adult female population density over the simulated period are illustrated in I. Panels A and B show

within-year changes in adult female population density, while G and H display correlation matrices between a subset of population-level outputs (x-axis) and individual-level traits (y-axis). Exemplary relationships are shown for the historic period between C) average longevity (in days) and peak adult abundance (count animals) and D) body condition (storage level as percent body fat) and peak offspring abundance (count animals). For the projected period, relationships are shown between E) litter size at weaning (count pups) and peak offspring abundance (count animals) and F) total metabolic rate (in kJ per day) and minimum adult population size (count animals). Densities in A, B, and I were collected at weekly intervals over each five-year period, with annual averages computed per simulation for I. Outputs in C–H were derived from averages of traits and population metrics recorded on six observation days per year (two each in spring, summer, and fall), totaling 30 days per time period per simulation. Correlations thus reflect broad time-period-level relationships, acknowledging that this resolution neglects within- and between-year variations. In A-F and I, colored points and lines represent outputs from each simulation replicate. In G and H, yellow represents negative and pink denotes positive correlations, determined via the Pearson correlation coefficient, with increasing saturation representing stronger effect size. Abbreviations used in G and H include: m = body mass (g), SL = storage level (% body fat), m_{neo} = neonate mass (g), m_{wean} = weaning mass (g), M_L = locomotion costs (J day^{-1}), M_R = reproduction costs (J day^{-1}), M_{LM} = cost of lean mass growth (J day^{-1}), M_{tot} = total metabolic rate (J day^{-1}), $age_{1st\ birth}$ = age at first birth (days), age_{death} = longevity (days), LPY = number of litters per year (N), LSW = litter size at weaning (N pups), LRS = lifetime reproductive success (N pups weaned), A_{peak} = peak adult abundance (N), TA_{peak} = timing of peak adult abundance (day of year), O_{peak} = peak offspring abundance (N), TO_{peak} = timing of peak offspring abundance (day of year), A_{min} = adult minimum abundance (N), and TA_{min} = timing of minimum adult abundance (day of year). Predictions were generated from 500 simulation runs, with thick lines representing generalized additive model (GAM) predictions in A and B and linear model predictions in C-F and I. For alternative scenarios, see Appendix Figures A2-6.